PAPER

# Compressed Sensing Framework Applying Independent Component Analysis after Undersampling for Reconstructing Electroencephalogram Signals*

**Daisuke KANEMOTO**[†a)], ***Member***, **Shun KATSUMATA**[††], **Masao AIHARA**[†††], ***Nonmembers***, ***and*** **Makoto OHKI**[††††], ***Member***

**SUMMARY** This paper proposes a novel compressed sensing (CS) framework for reconstructing electroencephalogram (EEG) signals. A feature of this framework is the application of independent component analysis (ICA) to remove the interference from artifacts after undersampling in a data processing unit. Therefore, we can remove the ICA processing block from the sensing unit. In this framework, we used a random undersampling measurement matrix to suppress the Gaussian. The developed framework, in which the discrete cosine transform basis and orthogonal matching pursuit were used, was evaluated using raw EEG signals with a pseudo-model of an eye-blink artifact. The normalized mean square error (NMSE) and correlation coefficient (CC), obtained as the average of 2,000 results, were compared to quantitatively demonstrate the effectiveness of the proposed framework. The evaluation results of the NMSE and CC showed that the proposed framework could remove the interference from the artifacts under a high compression ratio.

***key words:*** *EEG, compressed sensing, independent component analysis, random undersampling, artifact*

## 1. Introduction

Electroencephalogram (EEG) signals are important biometric signals used to reveal signs of brain inflammation, epilepsy [1], sleep disorders, and Alzheimer's disease [2]. Long-term wireless telemonitoring of EEG signals is required for accurately tracing brain activity. In general EEG wireless monitoring systems, sensors in the sensing unit are placed on the scalp, and EEG signals are transmitted wirelessly to a data processing unit, such as a workstation or a PC, for analysis. The data exchange in wireless communication requires large power consumption. Therefore, the energy efficiency of the sensing unit is important because its battery life is limited. Thus, a low-power sensing technique is required.

The compressed sensing (CS) theory, which is an attractive method for signal acquisition and compression [3], can enable the realization of a low-power sensing technique. This theory suggests that signals can be recovered from fewer measurements than required in the conventional Nyquist sampling technique, if the signal is sparse in some transform domains. However, if interferences from artifacts (from eye blinking, muscle activity, etc.) occur during EEG monitoring, the compressed signals become less sparse. Particularly, impulse noise strongly affects the quality of signal recovery [4].

On the other hand, independent component analysis (ICA) [5] has proved to be an effective algorithm for removing artifacts [6]–[8]. In some other studies, ICA was also performed to effectively separate only the desired information from the measured EEG signals before compressing the signals in a sensing unit [9]–[11]. Thus, performing ICA to improve sparsity before applying compression can be also considered. However, to perform ICA before undersampling, a micro-processing unit (MPU) that performs calculations must be installed in the sensing unit. This however this results in an increase in the power dissipation of the sensing unit owing to the additional implementation of the MPU. Therefore, it is not efficient to use ICA processing before undersampling for removing artifacts. Hence, we developed a new framework to remove artifacts from the compressed signals outside the sensing unit. The proposed framework does not require additional MPUs in the sensing unit to perform ICA.

This paper is organized as follows. Section 2 briefly describes the CS theory and ICA. Section 3 presents the details of the new framework. Section 4 presents the calculation results obtained with this proposed framework. In Sect. 5, we discuss the difference in reconstruction accuracy between two frameworks: ICA after compression (proposed framework) and ICA before compression. Section 6 presents the conclusions of the study. This paper is based on international conference proceedings [12].

Manuscript received May 1, 2020.
Manuscript publicized June 22, 2020.

[†]The author is with Division of Electrical, Electronic and Information Engineering, Osaka University, Suita-shi, 565-0871 Japan.
[††]The author is with Integrated Graduate School of Medicine, Engineering, and Agricultural Sciences, University of Yamanashi, Kofu-shi, 400-8511 Japan.
[†††]The author is with Graduate School of Medicine, University of Yamanashi, Kofu-shi, 400-8511 Japan.
[††††]The author is with Graduate Faculty of Interdisciplinary Research, University of Yamanashi, Kofu-shi, 400-8511 Japan.

*This paper is based on "Framework of Applying Independent Component Analysis After Compressed Sensing for Electroencephalogram Signals" by D.KANEMOTO, S.KATSUMATA, M.AIHARA, and M.OHKI which appeared in Proceedings of 2018 IEEE Biomedical Circuits and Systems Conference, October 2018. ©2018 IEEE.

a) E-mail: dkanemoto@eei.eng.osaka-u.ac.jp (Corresponding author)

DOI: 10.1587/transfun.2020EAP1058

## 2. CS Theory and ICA for EEG Signals

### 2.1 CS Theory for EEG Signals

The CS theory is utilized to solve the problem of obtaining a signal vector $\mathbf{x} \in \mathbb{R}^N$ of size $N$, which is $k$ -sparse in some basis matrix $\mathbf{\Psi} \in \mathbb{R}^{N \times P}$. $k$-sparse means that only $k(<< P)$ elements of the coefficient vector $\mathbf{s} \in \mathbb{R}^P$, used to show that $\mathbf{x} = \mathbf{\Psi}\,\mathbf{s}$, are nonzero. Using CS, we can obtain a compressed signal $\mathbf{y} = \mathbf{\Phi}\,\mathbf{x}$, where $\mathbf{\Phi}$ is the $M \times N$ measurement matrix. The compressed signal vector $\mathbf{y} \in \mathbb{R}^M$ can be written as

$$\mathbf{y} = \mathbf{\Phi x} = \mathbf{\Phi \Psi s} = \mathbf{\Theta s}. \tag{1}$$

Here, $\mathbf{y}$ is a known vector, and $\mathbf{\Phi}$ and $\mathbf{\Psi}$ are known matrices. $\mathbf{\Theta} = \mathbf{\Phi}\,\mathbf{\Psi}$ is called the sensing matrix. The relationship between $\mathbf{y}$ and $\mathbf{s}$ is shown in Fig. 1 using an example with $M$=5, $P$=20. The color depth indicates the numeric size of each element. White elements indicate zeros. The vector $\mathbf{s}$ is sparse and there are many zero elements. The length of $\mathbf{y}$ is much smaller than the length of $\mathbf{s}$. Therefore, we can understand from Fig. 1 that Eq. (1) is underdetermined. The most original approach for solving this problem is to find the sparsest vector. A solution is given by the following $l_0$ minimization problem:

$$\min ||\mathbf{s}||_0 \qquad \text{subject to} \qquad \mathbf{y} = \mathbf{\Theta s}. \tag{2}$$

It is well known that the $l_0$ minimization problem is NP-hard [13], and it cannot be used for practical applications. Therefore, other reconstruction algorithms (e.g. basis pursuit (BP) [14], orthogonal matching pursuit (OMP) [15], and block sparse Bayesian learning (BSBL) [16]) are widely used for solving CS problems. In general, there is a trade-off between the reconstruction time and accuracy. For example, it was reported that BP is better than OMP in terms of the reconstruction accuracy. However, the reconstruction time of BP tends to be longer owing to calculation complexities [17]. It was reported that BSBL is a powerful reconstruction tool for compressed EEG signals [16]. However, reconstruction using BSBL is more time consuming than that using OMP.

Determining the basis for EEG signal is also important to realize the sparsest vector. In some studies, discrete cosine transform (DCT) basis [16], Gabor basis [18], and wavelet basis [19] were used as $\mathbf{\Psi}$ in the reconstruction of compressed EEG signals. However, EEG signals are typically affected by artifacts. Therefore, it can become difficult to reconstruct the compressed signals clearly, because the measurement signals become less sparse in the above bases. Especially, it was reported that impulse noise affects the reconstruction of compressed data [4]. Thus, a new technique to recover signals from noisy measurements in CS system applications is desired.

The measurement matrix must be designed considering the hardware components and compatibility with the chosen basis. It is well known that a Gaussian matrix can be used as a classical measurement matrix $\mathbf{\Phi}$ (e.g., [9]). As an alternative, the random sampling matrix, which is realized using a low-rate random undersampling analog-to-digital (A/D) converter, was developed [20].

The design of a data acquisition system in which CS is applied, requires specific consideration of the reconstruction algorithm, basis, and measurement matrix that should be selected. For example, reconstruction algorithms have a trade-off relationship between the reconstruction time and reconstruction accuracy. We also have to find a suitable sensing matrix, which can transform to the sparsest vector. Therefore, selecting the appropriate reconstruction algorithm, basis, and measurement matrix depends on the application and type of the target signal. In this study, taking EEG measurement application as an example, we used OMP as the reconstruction algorithm and DCT as the basis to evaluate our proposed framework. The measurement matrix will be discussed later in this paper.

### 2.2 ICA for EEG Signals

From the ICA model, the measured $L$-channel EEG signals $\mathbf{D}$=$[d_1(t),\cdots,d_{L-1}(t),d_L(t)]^{\mathrm{T}}$ may be considered as a linear combination of $L$ unknown underlying sources $\mathbf{E}$ =$[e_1(t),\cdots,e_{L-1}(t),e_L(t)]^{\mathrm{T}}$, with

$$\mathbf{D} = \mathbf{HE}, \tag{3}$$

where

$$\mathbf{H} = \begin{bmatrix} h_{11} & \cdots & h_{1L} \\ \vdots & \ddots & \vdots \\ h_{(L-1)1} & \cdots & h_{(L-1)L} \\ h_{L1} & \cdots & h_{LL} \end{bmatrix}, \tag{4}$$

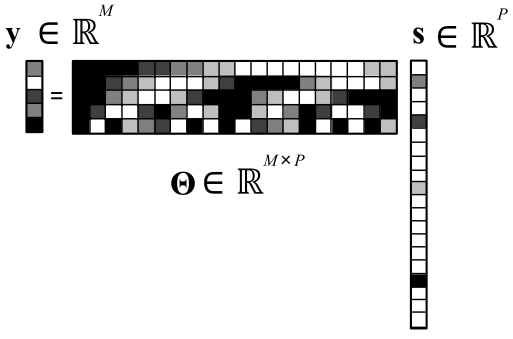


**Fig. 1** Relationship between $\mathbf{y}$ and $\mathbf{s}$.

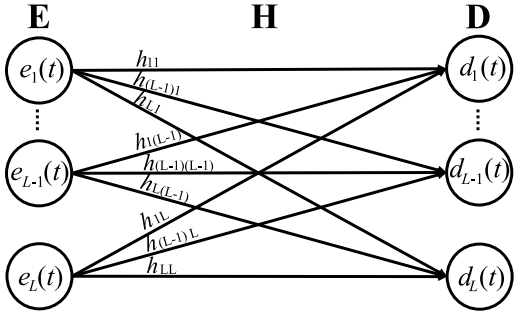


**Fig. 2** Linear mixture model.

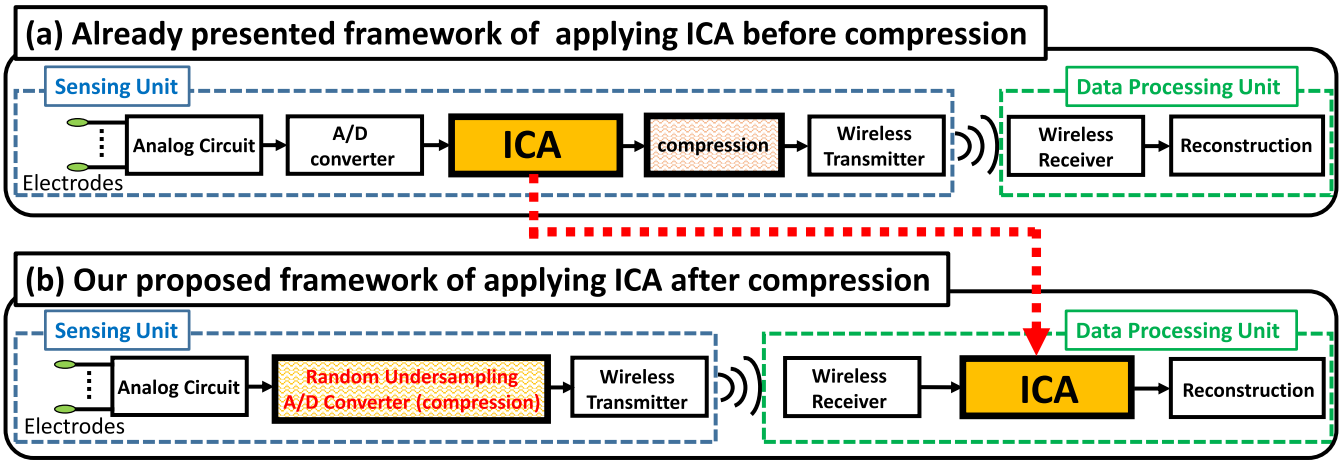


**Fig. 3** EEG measurement frameworks. (a) ICA before compression (b) ICA after compression (proposed framework) ©2018 IEEE.

is the unknown mixing matrix (Fig. 2). The goal of ICA is to estimate $\mathbf{E}$ from the given $\mathbf{D}$. We can calculate the estimated sources by obtaining the unmixing matrix $\widehat{\mathbf{W}}$, where $\widehat{\mathbf{W}} = \mathbf{H}^{-1}$. In some EEG studies, ICA is used to remove artifacts [6]–[8]. However, in general, ICA relies on the assumption that $\mathbf{E}$ is not Gaussian because $\widehat{\mathbf{W}}$ becomes unidentifiable [5]. Thus, it is difficult to separate the data, which are compressed using a Gaussian measurement matrix.

## 3. Proposed Framework

Figure 3 shows the existing framework (ICA before compression) and our proposed EEG measurement framework (ICA after compression) [12]. These frameworks are primarily composed of two parts: ICA processing part and CS part. Figure 3(a) shows the existing framework in which the desired information can be separated from the measured signals effectively before compression to reduce the amount of data [9]–[11]. However, a power consumption problem occurs if we add digital processing in the sensing unit such as that in ICA. Therefore, we developed a fundamentally new framework to solve this problem (Fig. 3(b)). In this framework, additional power-consuming processing components are not required in the sensing unit, owing to the application of ICA in the data processing unit. The details of both units in our proposed framework are given below.

### 3.1 Sensing Unit in Our Proposed Framework

Figure 4 shows the details of the sensing unit used in $L$-channel EEG measurements. In actual EEG measurements, artifacts are present in the measured signals. Here, $\mathbf{x}_{\text{Ch-}i}$ and $\mathbf{a}_{\text{Ch-}i}$ indicate the measured pure EEG signals and artifacts in $i$-th channel, respectively. The length of each signal is presented as $N$. Initially, these signals are appropriately processed in an analog circuit block. Subsequently, $L$ random sampling A/D converters perform undersampling of the signals, $\mathbf{x}_{\text{Ch-}i} + \mathbf{a}_{\text{Ch-}i}$, to achieve $M$ data from $N$ data. The

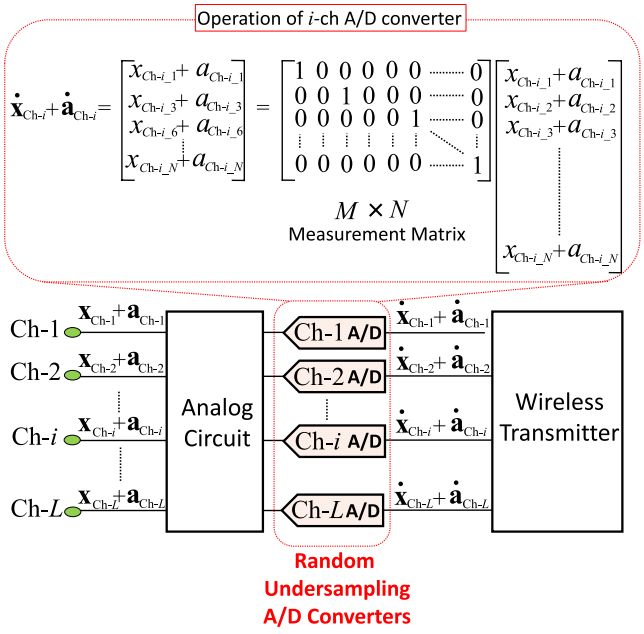


**Fig. 4** Sensing unit in our framework. ©2018 IEEE.

measurement matrix is presented at the top of Fig. 4. The random sampling technique introduced in [20] is used to compress the measured EEG signal in the sensing unit; this is to avoid the problem in which ICA is difficult to apply for separating signals following a Gaussian distribution [5]. In actual A/D converters, the input signals are quantized. Thus, we have to determine the appropriate resolution for A/D converters. However, in this study, resolution was not considered, and we used the A/D converters as samplers to explain the principle of our proposed framework. In each row of the $M \times N$ measurement matrix in the A/D converter, only one element is "1" and the others are all "0." The compressed signals, $\dot{\mathbf{x}}_{\text{Ch-}i} + \dot{\mathbf{a}}_{\text{Ch-}i}$, are transferred to the data processing unit through a wireless transmitter.

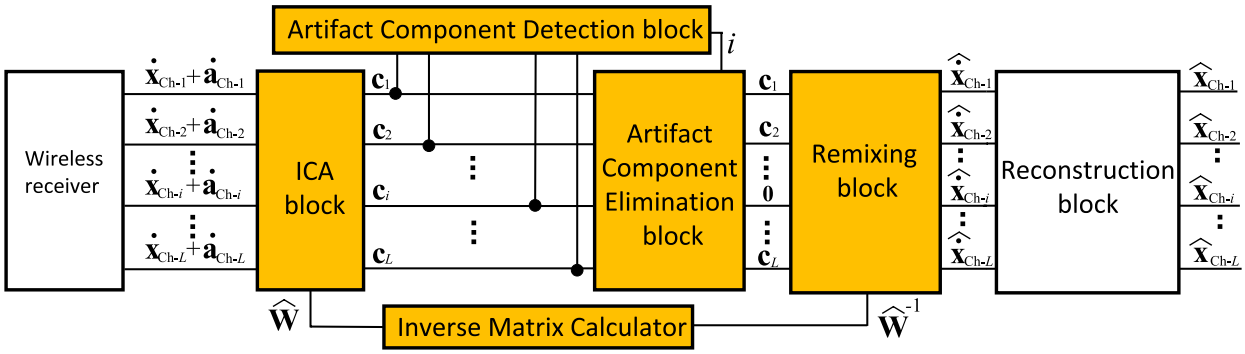


**Fig. 5** Data processing unit in our framework. ©2018 IEEE.

### 3.2 Data Processing Unit in Our Proposed Framework

Figure 5 shows the block diagram of the data processing unit. The compressed data, $\dot{\mathbf{x}}_{\text{Ch-}i} + \dot{\mathbf{a}}_{\text{Ch-}i}$, are received through a wireless receiver. Subsequently, ICA is performed in the ICA block to generate $L$ components from $\mathbf{c_1}$ to $\mathbf{c_L}$, and the unmixing matrix $\widehat{\mathbf{W}}$. Next, the component representing an artifact is revealed in the artifact component detection block. We assumed that the $i$-th component indicated the artifact. Next, all data of the $i$-th component are reduced to 0 in the artifact component elimination block. Finally, the estimated EEG signal of each channel from $\widehat{\mathbf{x}}_{\text{Ch-1}}$ to $\widehat{\mathbf{x}}_{\text{Ch-}L}$ can be achieved using the compressed signals from $\widehat{\dot{\mathbf{x}}}_{\text{Ch-1}}$ to $\widehat{\dot{\mathbf{x}}}_{\text{Ch-}L}$ in the CS reconstruction block.

## 4. Evaluation

We evaluated our framework using the measured EEG signals. The measured raw EEG signals, which were recorded at 200 Hz in 16 channels ($L$=16) at a hospital, were used as the input EEG signals for the measurement frameworks. The time corresponding to one epoch was 3 s. The evaluation was performed using MATLAB software. The model encompassed the EEG signal acquisition in the sensing unit to data reconstruction in the data processing unit. To focus on the verification of our framework operation, the analog circuit adopted an ideal model in all verification results. Eye-blink artifacts are the most common artifacts that easily interfere with EEG measurements. Therefore, we generated a pseudo-model of eye-blink artifacts to evaluate the extent to which these artifacts were eliminated in our proposed framework.

Several shapes of eye-blink artifact in EEG signals have been reported and the shapes differ by subject [21]. Therefore, we used a simple model of an impulse and triangular shaped eye-blink artifact (e.g. [22]) in this paper. It has also been reported that the period and magnitude of an eye-blink artifact depend on the subject. For example, it was reported that the distortion of the EEG caused by an eye-blink lasts longer than 100 ms [21]. The range is approximately between 50 $\mu$V and 250 $\mu$V of the magnitude, as shown in [22]. In some papers, the received magnitude of the eye-blink artifacts near the eye electrodes is larger than that at the other parts. Further, it is well known that eye-blink artifacts decrease rapidly with an increase in distance from the eyes (e.g. [23]).

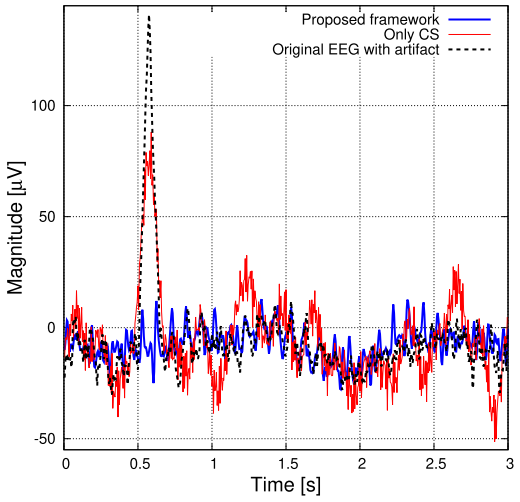


**Fig. 6** EEG signals (Original with artifact, only CS, and proposed framework). As an example, $k$ = 20 was used. ©2018 IEEE.

Based on the above information and our EEG measurement experience, a pseudo-model of the eye-blink artifact was created and used for evaluation. The maximum voltage of the pseudo-model of the eye-blink artifact was set as 150 $\mu$V in the electrodes FP1 and FP2. The peaks of the artifacts in F3, F4, F7, and F8 correspond to 75 $\mu$V. In the other electrodes (C3, C4, P3, P4, T3, T4, T5, T6, O1, and O2), artifacts with a voltage of 15 $\mu$V were added to the measured EEG signals. In this evaluation, we used the principal component analysis (PCA)–ICA algorithm [24] in the ICA block. OMP was used in the reconstruction block, in which the sparse parameter $k$ was set at 20 as an example. The DCT basis was used as $\mathbf{\Psi}$.

Figure 6 shows the examples of the original signal with the pseudo-model of the eye-blink artifacts and the reconstructed signal by using the proposed framework at FP1. Figure 6 also shows the results obtained using only CS. The compression ratio (CR = $N/M$) is 4 during the evaluation using only CS and the proposed framework. A pseudo-model artifact was inserted from 0.5 s to 0.65 s in the original

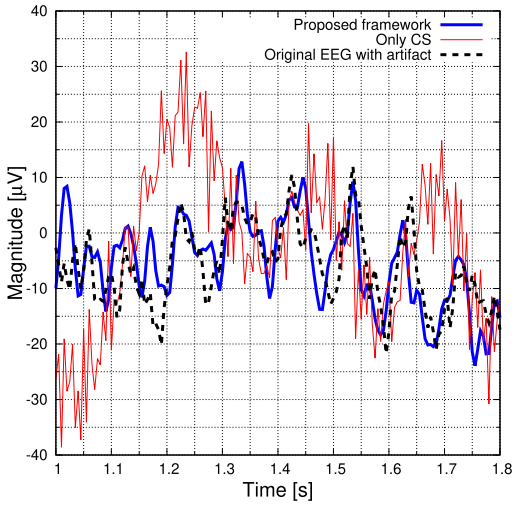


**Fig. 7** EEG signals (zoomed-in view of Fig. 6) ©2018 IEEE.

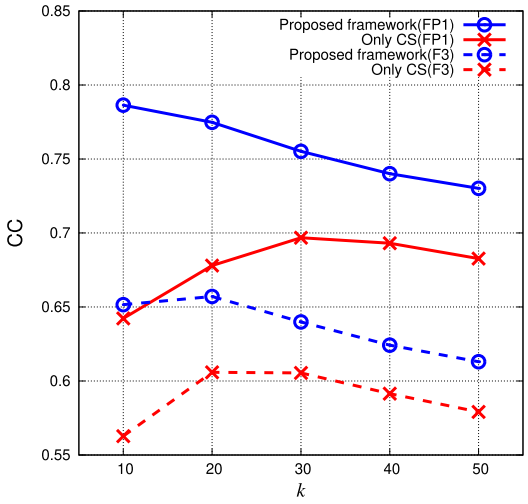


**Fig. 9** CC with various $k$ values at FP1 and F3.

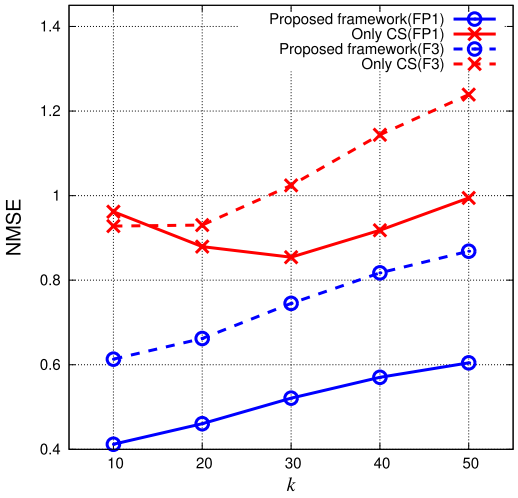


**Fig. 8** NMSE with various $k$ values at FP1 and F3.

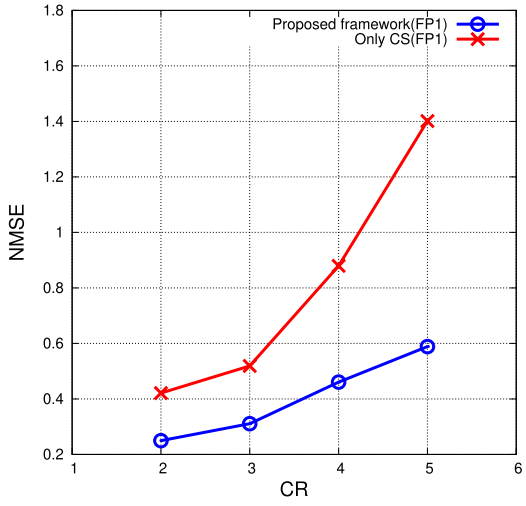


**Fig. 10** NMSE with various CRs at FP1.

data. Using our framework, the artifact could be removed effectively when compared with that using only CS. Figure 7 shows the zoomed-in view of Fig. 6 from 1.0 s to 1.8 s. These results indicate successful reconstruction of the EEG waveform using our proposed framework.

To evaluate the performance of the proposed framework, we used two different performance indices. One is the normalized mean square error (NMSE) that normalizes the average of the square of the difference between the estimated and original values. It was calculated as follows:

$$\mathrm{NMSE} = \frac{\|\mathbf{x} - \hat{\mathbf{x}}\|_2^2}{\|\mathbf{x}\|_2^2}, \tag{5}$$

where $\mathbf{x}$ is the original EEG signal and $\hat{\mathbf{x}}$ is the reconstructed EEG signal. $\|\cdot\|_2$ denotes the Euclidean norm. Another performance index is the correlation coefficient (CC), which measures the similarity between two waveforms. It was calculated as

$$\mathrm{CC} = \frac{S_{\mathbf{x}\hat{\mathbf{x}}}}{S_{\mathbf{x}} S_{\hat{\mathbf{x}}}}, \tag{6}$$

where $S_{\mathbf{x}\hat{\mathbf{x}}}$ is the covariance between $\mathbf{x}$ and $\hat{\mathbf{x}}$, and $S_{\mathbf{x}}$ and $S_{\hat{\mathbf{x}}}$ are the standard deviations of $\mathbf{x}$ and $\hat{\mathbf{x}}$, respectively. We evaluated the NMSE and CC at CR=4 with various values of $k$ ranging from 10 to 50. Figure 8 shows the calculated NMSE values at FP1 and P3. We prepared 10 types of measurement matrices in which the positions of "1" were different. Therefore, we calculated the NMSE values by averaging the results 2,000 times (= 200 epochs × 10 times simulation results with 10 types of measurement matrices). In these results, we ignored the data from 0.5 s to 0.65 s, in which the results obtained using only CS were strongly affected by the artifacts; we did so to perform a fair comparison between the results obtained using the proposed framework and those obtained with only CS. We observed that the NMSE values obtained using the proposed framework were lower than those obtained using only CS for any value of $k$. For example, at $k = 20$ shown in Fig. 8, the NMSE obtained using

only CS is approximately 0.88 although the NMSE obtained using the proposed framework is below 0.48 at FP1. Figure 9 shows the CC evaluation results at FP1 and P3. These values are also the averages of 2,000 results. With CR=4, we could achieve higher-quality reconstructed signals with any $k$ value in comparison with that possible using only CS. Figure 10 shows the relationship between the NMSE and various CR with $k = 20$ at FP1. The result was obtained through 2,000-times averaging. Overall, as CR increases, the NMSE increases. We can observe that the NMSE obtained using the proposed framework is smaller than that obtained using only CS at any CR. Thus, based on the above evaluations, we concluded that our framework could remove the interference from artifacts under a high CR.

## 5. Discussion

In the discussion presented up to Sect. 4, it was mentioned that the proposed framework is capable of signal reconstruction owing to the suppression of the influence of artifacts, even if the MPU is not installed in the sensing unit. In this section, we discuss the differences in the reconstruction accuracy between the two frameworks: ICA after compression (proposed framework) and ICA before compression (e.g. [9]–[11]). The most important difference in both frameworks is where the ICA is operated. In ICA before compression, the artifact component can be separated from uncompressed measurement EEG signals (i.e., from $\mathbf{x}_{\text{Ch-}i} + \mathbf{a}_{\text{Ch-}i}$ to $\mathbf{x}_{\text{Ch-}i}$ and $\mathbf{a}_{\text{Ch-}i}$). This is a typical method that applies ICA to EEG signals, and there are many papers which show artifact separation successfully(e.g. [6]). On the other hand, in the proposed framework, ICA is applied to compressed measurement EEG signals (i.e., $\dot{\mathbf{x}}_{\text{Ch-}i} + \dot{\mathbf{a}}_{\text{Ch-}i} = \mathbf{\Phi}(\mathbf{x}_{\text{Ch-}i} + \mathbf{a}_{\text{Ch-}i})$). Therefore, the reconstruction accuracy of the proposed framework depends on whether the ICA can separate compressed measurement EEG signals for independent components correctly. Based on the above discussion, we note that the measurement matrix is particularly important.

To separate independent components using ICA, the components obtained by decomposition should be statistically independent and non-Gaussian [5]. When the random undersampling matrix is used as the measurement matrix, the original data are only thinned out, and the independence of the original data is not affected. In addition, as explained in Sect. 3.1, avoiding a Gaussian distribution of independent components can be also realized using random undersampling matrix as the measurement matrix, which is different from the Gaussian measurement matrix. From the above, we found that the compressed measurement EEG signals and artifacts can be separated in the proposed framework, theoretically.

Next, the difference between the existing ICA before compression framework, in which MPUs are required in the sensing unit, and the proposed framework was evaluated using CC. The evaluation was performed under the same conditions as described in Sect. 4 (i.e., using OMP as the reconstruction algorithm, PCA–ICA as the ICA algorithm,

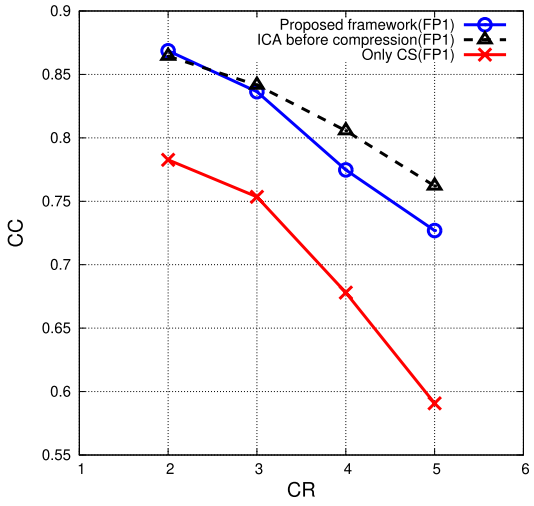


**Fig. 11** CC evaluation results by using OMP, PCA–ICA at FP1 (proposed framework (ICA after compression), ICA before compression framework, and only CS.

and averaging the results 2,000 times). Figure 11 shows the evaluation results with the proposed framework (ICA after compression), ICA before compression framework, and only CS at FP1. From Fig. 11, it can be seen that up to CR = 3, a reconstruction accuracy of the proposed framework as high as ICA before compression framework can be achieved. When CR = 4 or more, there are slight differences in the reconstruction accuracy; however, it is clear that the proposed framework can recover with a higher accuracy than only CS, although the proposed framework does not need MPUs to operate ICA in the sensing unit. If a higher reconstruction accuracy is desired, then an additional signal processing can be accepted in the data processing unit; for example, applying an additional method for removing artifacts efficiently [25] is also one solution.

## 6. Conclusion

We developed a new framework for reconstructing EEG signals affected by artifacts. The sensing unit in our framework does not require ICA to suppress the artifacts, and the ICA block can be moved to the data processing unit. Therefore, we can remove the additional digital processing functions in the sensing unit. In this framework, we used the random undersampling measurement matrix in CS to perform ICA for suppressing the Gaussian. The proposed framework was evaluated on MATLAB using 3-s 16-channel raw EEG signals with a pseudo-model of the eye-blink artifact. In the evaluation, a combination of OMP as the reconstruction algorithm, DCT basis, and the PCA–ICA algorithm was used. The NMSE and CC values were compared to quantitatively evaluate the effectiveness of our proposed framework. For example, the NMSE obtained using only CS was approximately 0.88 although that obtained using the proposed framework was below 0.48 with CR=4 at FP1. The evaluation results showed that the framework could remove the

interference from artifacts under a high CR without using MPUs in the sensing unit.

## Acknowledgments

This work was supported by JSPS KAKENHI Grant Number JP18K18023, Adaptable and Seamless Technology Transfer Program through Target-driven R&D (A-STEP) from Japan Science and Technology Agency (JST), and JKA foundation. The authors would like to thank the staff at the University of Yamanashi Hospital for their helpful suggestions and technical assistance with EEG data collection.

### References

[1] H.R. Mohseni, A. Maghsoudi, and M.B. Shamsollahi, "Seizure detection in EEG signals: A comparison of different approaches," Proc. IEEE Engineering in Medicine and Biology Society, pp.6724–6727, Sept. 2006.
[2] T. Musha, H. Matsuzaki, Y. Kobayashi, Y. Okamoto, M. Tanaka, and T. Asada, "EEG markers for characterizing anomalous activities of cerebral neurons in NAT (neuronal activity topography) method," IEEE Trans. Biomed. Eng., vol.60, no.8, pp.2332–2338, Aug. 2013.
[3] D. Gangopadhyay, E.G. Allstot, A.M.R. Dixon, K. Natarajan, S. Gupta, and D.J. Allstot, "Compressed sensing analog front-end for bio-sensor applications," IEEE J. Solid-State Circuits, vol.49, no.2, pp.426–438, Feb. 2014.
[4] X. Zou, L. Feng, and H. Sun, "Robust compressive sensing of multichannel EEG signals in the presence of impulsive noise," Information Sciences, vol.429, pp.120–129, March 2018.
[5] A. Hyvärinen, J. Karhumen, and E. Oja, Independent Component Analysis, John Wiley & Sons, 2001.
[6] N.P. Castellanos and V.A. Makarov, "Recovering EEG brain signals: Artifact suppression with wavelet enhanced independent component analysis," J. Neurosci. Meth., vol.158, no.2, pp.300–312, Dec. 2006.
[7] S. Makeig, A.J. Bell, T. Jung, and T.J. Sejnowski, "Independent component analysis of electroencephalographic data," Advances in Neural Information Processing Systems, pp.145–151, Aug. 1996.
[8] S. Çınar, N. Acır, "A novel system for automatic removal of ocular artefacts in EEG by using outlier detection methods and independent component analysis," Expert Syst. Appl., vol.68, pp.36–44, Feb. 2017.
[9] B. Zhou, X. Wu, Z. Lv, L. Zhang, and C. Zhang, "Independent component analysis combined with compressed sensing for EEG compression in BCI," Proc. International Conference on Information, Communications and Signal Processing, pp.1–4, Dec. 2015.
[10] B. Mijović, V. Matić, M. De Vos, and S. Van Huffel, "Independent component analysis as a preprocessing step for data compression of neonatal EEG," Proc. IEEE Engineering in Medicine and Biology Society, pp.1–5, Aug. 2011.
[11] S. Fauvel, A. Agarwal, and R. Ward, "Compressed sensing and energy-aware independent component analysis for compression of EEG signal," Proc. IEEE International Conference on Acoustics, Speech and Signal Processing, pp.973–977, May 2013.
[12] D. Kanemoto, S. Katsumata, M. Aihara, and M. Ohki, "Framework of applying independent component analysis after compressed sensing for electroencephalogram signals," Proc. 2018 IEEE Biomedical Circuits and Systems Conference, pp.145–148, Oct. 2018.
[13] B.K. Natarajan, "Sparse approximate solutions to linear systems," SIAM J. Comput., vol.24, no.2, pp.227–234, April 1995.
[14] D. Donoho, "Compressed sensing," IEEE Trans. Inf. Theory, vol.52, no.4, pp.1289–1306, April 2006.
[15] J.A. Tropp and A.C. Gilbert, "Signal recovery from random measurements via orthogonal matching pursuit," IEEE Trans. Inf. Theory, vol.53, no.12, pp.4655–4666, Dec. 2007.
[16] Z. Zhang, T. Jung, S. Makeig, and B.D. Rao, "Compressed sensing of EEG for wireless telemonitoring with low energy consumption and inexpensive hardware," IEEE Trans. Biomed. Eng., vol.60, no.1, pp.221–224, Jan. 2013.
[17] A.M. Abdulghani, A.J. Casson, and E. Rodriguez-Villegas, "Compressive sensing scalp EEG signals: Implementations and practical performance," Med. Biol. Eng. Comput., vol.50, no.11, pp.1137–1145, Nov. 2012.
[18] M. Mohsina and A. Majumdar, "Gabor based analysis prior formulation for EEG signal reconstruction," Biomedical Signal Processing and Control, vol.8, no.6, pp.951–955, Nov. 2013.
[19] L. Lin, Y. Meng, J.P. Chen, and Z.B. Li, "Multichannel EEG compression based on ICA and SPIHT," Biomedical Signal Processing and Control, vol.20, pp.45–51, April 2015.
[20] J. Laska, S. Kirolos, Y. Massoud, R. Baraniuk, A. Gilbert, M. Iwen, and M. Strauss, "Random sampling for analog-to-information conversion of wideband signals," Proc. IEEE Dallas/CAS Workshop Design, Applications, Integration and Software, pp.119–122, Oct. 2006.
[21] I. Erkens and G.G. Molina, "Artifact detection and correction in Neurofeedback and BCI applications," Philips Research, Tech. note TN-PR 2008/00409, 2008.
[22] W.D. Chang, H.S. Cha, K. Kim, and C.H. Im, "Detection of eye blink artifacts from single prefrontal channel electroencephalogram," Comput. Meth. Prog. Bio., vol.124, pp.19–30, Feb. 2016.
[23] V. Krishnaveni, S. Jayaraman, S. Aravind, V. Hariharasudhan, and K. Ramadoss, "Automatic identification and removal of ocular artifacts from EEG using wavelet transform," Measurement Science Review, vol.6, no.4, pp.45–57, 2006.
[24] K. Zhang and L. Chan, "ICA by PCA approach: Relating higher-order statistics to second-order moments," Proc. International Conference on Independent Component Analysis and Signal Separation, pp.311–318, March 2006.
[25] S. Katsumata, D. Kanemoto, and M. Ohki, "Applying outlier detection and independent component analysis for compressed sensing EEG measurement framework," Proc. 2019 IEEE Biomedical Circuits and Systems Conference, pp.1–4, Oct. 2019.

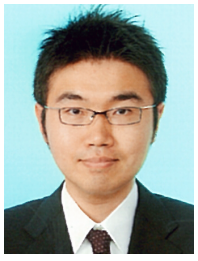

**Daisuke Kanemoto** received his B.S. degree in Electronics and Information Science from Kyoto Institute of Technology, Kyoto, Japan, in 2004 and M.S. and Ph.D. degrees in Electronic Engineering from Osaka University, Osaka, Japan, in 2006, 2011. From 2010 to 2013, he was an assistant professor in the Department of Electronics, Graduate School of Information Science and Electrical Engineering, Kyushu University, Fukuoka, Japan. From 2013 to 2019, he was an assistant professor in the Department of Research Interdisciplinary Graduate School of Medicine and Engineering, University of Yamanashi, Yamanashi, Japan. From 2015 to 2017, he was a visiting assistant professor in the Department of Electrical Engineering, Stanford University, Stanford, USA. From 2019, he has been an associate professor with Graduate School of Engineering Osaka University, Osaka, Japan. His research interests include analog circuits, mixed-signal integrated circuits and compressed sensing. He is an IEEE member.

**Shun Katsumata** received his B.S. degree from the University of Yamanashi, Japan, in 2018. Since 2018, he has been a master's student in the Integrated Graduate School of Medicine, Engineering, and Agricultural Sciences, University of Yamanashi, Yamanashi, Japan. His research interests are compressed sensing and independent component analysis for EEG.

**Masao Aihara** received his M.D. and Ph.D. degrees from Chiba University, Chiba, Japan, in 1981 and 1988, respectively. Presently, he is a Professor in the Graduate Faculty of Interdisciplinary Research, Graduate School, University of Yamanashi. His research interest is the cognitive neuroscience of frontal lobe functions in children and developmental disorders.

**Makoto Ohki** received his B.E. degree from University of Yamanashi, Kofu, Japan, in 1985, and M.E. and D.E. degrees from Tohoku University, Sendai, Japan, in 1987 and 1990, respectively, all in electronic engineering. He is currently a professor with University of Yamanashi, Kofu, Japan. His research interests include multidimensional signal processing and adaptive signal processing.